Structure and selfdiffusion in a model twodimensional Brownian liquid

H. ArandaEspinoza, M. CarbajalTinoco, E. UrrutiaBañuelos, J. L. ArauzLara, M. MedinaNoyola, and J. Alejandre

Citation: The Journal of Chemical Physics **101**, 10925 (1994); doi: 10.1063/1.467842
View online: http://dx.doi.org/10.1063/1.467842
View Table of Contents: http://scitation.aip.org/content/aip/journal/jcp/101/12?ver=pdfcov
Published by the AIP Publishing

Structure and self-diffusion in a model two-dimensional Brownian liquid

H. Aranda-Espinoza, M. Carbajal-Tinoco, E. Urrutia-Bañuelos, J. L. Arauz-Lara, and M. Medina-Noyola
Instituto de Física "Manuel Sandoval Vallarta," Universidad Autónoma de San Luis Potosí, Apartado Postal 629, 78000 San Luis Potosí, S.L.P., México

J. Alejandre
Departamento de Química, Universidad Autónoma Metropolitana-Iztapalapa, Apartado Postal 55-534, 09340 México, D.F., México

(Received 27 July 1994; accepted 13 September 1994)

The static structure and the time-dependent self-diffusion motion of interacting Brownian particles in a model two-dimensional suspension are discussed. For the static structure we report Brownian dynamics results assuming a hard disk plus Yukawa pair potential. The self-diffusion properties of this model system are calculated from two independent theoretical approaches. In order to assess the accuracy of the predictions of these two theories, we also performed Brownian dynamics calculations of the time-dependent self-diffusion coefficient for a wide range of values of both the particle concentration and the pair potential coupling constant. We find that both theories reproduce very well the main features exhibited by the Brownian dynamics data. Quantitatively, there are some discrepancies between both theoretical predictions and the Brownian dynamics results, which are negligible at moderate couplings, but become larger for strongly coupled systems and long times. © *1994 American Institute of Physics.*

I. INTRODUCTION

The static and dynamic properties of suspensions of interacting colloidal particles have been studied rather extensively over the last 15 years.[1–3] The progress achieved in these years has been based on the application of sound theoretical approaches,[1–5] careful experimental measurements,[1–2,6] and adequate computer simulations.[7] A successful encounter of these three approaches has also been the result of the selection of well-characterized model systems, both from the experimental and from the theoretical point of view.[1,6] It is fair to say, for example, that at least for monodisperse suspensions of dilute but highly charged colloidal particles, a satisfactory description exists of their most fundamental properties. Thus, theoretical predictions of their static and dynamic properties, such as the static structure factor, self-diffusion coefficient, mean-squared displacement, etc., have been successfully compared with both, computer simulations and experimental results.[6]

The comments above refer mainly to monodisperse suspensions in the absence of external fields, and in unrestricted three-dimensional space. This research is currently being extended, among various directions, to study colloidal mixtures,[8] or the effects of static external fields, particularly those produced by confining walls, on the structural and dynamic properties of a colloidal suspension.[9] In this manner, for example, the continuous transition between a three-dimensional system to an effective two-dimensional suspension (a monolayer of colloidal particles confined by two flat surfaces) has been studied. As a result, a number of important experimental observations have been made concerning the phase behavior, structure, and dynamics of such two-dimensional Brownian liquid. This progress calls for the corresponding development of a theoretical description similar to what has been developed in the context of three-dimensional suspensions.[6] The aim of the work reported here is to contribute to this general line of research.[10]

Here we present the extension to two dimensions, of two approximate theories of self-diffusion in monodisperse suspensions in the absence of hydrodynamic interactions, and compare their predictions with the results obtained from Brownian dynamics (BD) computer simulations. One of these theories[11] is based on the generalized Langevin equation formalism, within the approximation scheme referred to[12] as *Fick plus decoupling approximation* (FDA). The main result of this theory is an expression for the time-dependent friction function $\Delta\zeta(t)$ in terms of the static structure factor of the suspension. From this function, one can calculate self-diffusion properties such as the mean squared displacement, velocity autocorrelation function, and self-diffusion coefficient.

These properties can also be written in terms of the memory function $M(k,t)$ of the time-evolution equation of the self-diffusion propagator.[3] The second theory we apply here to our two-dimensional model suspension is referred to[4,5] as *single exponential approximation* (SEXP), and assumes this functional form for the memory function $M(k,t)$, which is finally written in terms of the radial distribution function of the system. The main feature of these two theories is that they lead to expressions for self-diffusion properties in terms only of static quantities. Thus, this static input must first be available if quantitative predictions are to be obtained. Since the Brownian dynamics simulations yield both static and dynamic information, one can use the simulated static structure to calculate the predictions of these two theories for the dynamic properties. These predictions can then be compared with the dynamic results obtained directly from the Brownian dynamics experiment. This is essentially what we do in the work reported here.

Previously, the two dynamic theories referred to above were applied successfully to *three-dimensional* suspensions.

In the first stage of such application, the consistency between the predictions of the two theories was assessed, followed by a comparison with available computer simulation data.[5] As a result, it was found that both theories described essentially the same general behavior concerning the main features of dynamic properties such as the mean squared displacement and self-diffusion coefficient. The comparison with computer simulations confirmed the qualitative accuracy of the features predicted, and established the level of their quantitative accuracy. Later on, the same two theories were successfully employed in one of the most precise comparisons of theoretical results with experimental time-dependent data for self-diffusion properties.[6] This work then pretends to be the first step in a similar program, now developed in the context of the study of a two-dimensional Brownian liquid.

In this work we calculate the time-dependent self-diffusion properties of a rather idealized and arbitrary model suspension. This suspension is characterized by a short time self-diffusion coefficient D_0, which describes the Brownian motion in the absence of interactions (i.e., at zero concentration of colloidal particles). No attempt is made to calculate or assume any specific dependence of this free-diffusion coefficient in terms of parameters such as the viscosity of the solvent, or the particle size, as the Stokes–Einstein expression does for three-dimensional suspensions. Instead, D_0 is taken here as an elementary parameter in terms of which the self-diffusion properties describing the effects of the direct interactions will be expressed. The effects of hydrodynamic interactions will not be discussed at all. It is not because we assume that these or other possible effects (such as those produced by confining walls) are not important for a particular experimental system. The main reason is that most of these effects will be quite specific, and should be studied in the context of well-defined particular experimental conditions. From the theoretical point of view, it is important to understand first the effects of collisions and direct interactions between particles which undergo Brownian motion in the simplest general conditions, and this is why in this stage we do not commit yet to any specific experimental system. For the same reason, we have chosen a model for the direct interactions in a rather arbitrary manner. The hard-core plus Yukawa potential has been widely studied in the context of three-dimensional systems,[3–6] and one would like to be able to compare the self-diffusion properties of the same model in two and in three dimensions. A quantitative study of these dynamic properties, at least within the framework of the theories discussed here, requires the previous determination of the static properties of the system. Thus, an essential aspect of the present study is the development of a quantitative description of these static properties. Because of its intrinsic interest, here we devote a full section to the detailed discussion of this subject.

In the following section, a number of general definitions are summarized, and the two theories of self-diffusion referred to above are described. We also include a brief description of our BD calculations. Section III contains a fairly detailed account of the salient features of the static properties of the two-dimensional hard-disk plus Yukawa fluid, and Sec. IV presents and compares the specific results for the time-dependent self-diffusion properties predicted by the two theories described below and the corresponding results from BD. A summary and discussion of results are found in Sec. V.

II. GENERAL CONCEPTS AND DEFINITIONS

The property of main interest in this paper is the mean-squared displacement $W(t)$ of a labeled particle, or equivalently, the time-dependent self-diffusion coefficient, $D(t)$, defined (for our two-dimensional system) as

$$D(t)\equiv\frac{W(t)}{t}\equiv\langle[\Delta\mathbf{r}(t)]^2\rangle/4t, \tag{1}$$

where $\Delta\mathbf{r}(t)$ is the displacement of the particle during a time t. This property may be obtained from the velocity autocorrelation function (VAF)

$$V(t)\equiv\langle\mathbf{v}(0)\cdot\mathbf{v}(t)\rangle/2, \tag{2}$$

in which $\mathbf{v}(t)$ is the particle's velocity, by means of the exact relationship

$$D(t)=\int_0^t dt'(1-t'/t)V(t'). \tag{3}$$

The long-time limit of $D(t)$ is the self-diffusion coefficient D_s,

$$D_s\equiv\lim_{t\to\infty}D(t)=\int_0^\infty dt'\ V(t'). \tag{4}$$

In its turn, the velocity autocorrelation function may be written in terms of another fundamental property, which is the time-dependent friction function $\Delta\zeta(t)$. Thus, let us describe the Brownian motion of the labeled particle by the following generalized Langevin equation[10]

$$M\frac{d\mathbf{v}(t)}{dt}=-\zeta^0\mathbf{v}(t)+\mathbf{f}(t)-\int_0^t\Delta\zeta(t-t')\mathbf{v}(t')dt' + \mathbf{F}^{\rm int}(t), \tag{5}$$

where M is the particle's mass, ζ^0 is the friction coefficient in the absence of direct interactions (defined here in terms of D_0 as $\zeta^0=k_BT/D_0$), and $\mathbf{f}(t)$ is its corresponding white random force. Then, $\mathbf{F}^{\rm int}(t)$ is the colored random force exerted by the other particles on the labeled particle as their distribution departs instantaneously from its radial equilibrium average. The time-dependent correlation function of $\mathbf{F}^{\rm int}(t)$ is related to the (time-dependent) friction coefficient by the following fluctuation–dissipation relation:[11]

$$\Delta\zeta(t)=\beta\langle\mathbf{F}^{\rm int}(0)\cdot\mathbf{F}^{\rm int}(t)\rangle/2, \tag{6}$$

where $\beta=1/k_BT$, T being the temperature and k_B being Boltzmann's constant. The velocity autocorrelation function $V(t)$ then solves the same equation [Eq. (5)], without the random terms, whose solution is

$$\tilde{V}(z)=\frac{k_BT/M}{z+\dfrac{\zeta^0}{M}+\dfrac{\Delta\tilde{\zeta}(z)}{M}}. \tag{7}$$

Here the tilde indicates Laplace transform,

$$\tilde{V}(z)\equiv\int_0^\infty e^{-zt}V(t)dt, \tag{8}$$

$$\Delta\tilde{\zeta}(z)\equiv\int_0^\infty e^{-zt}\Delta\zeta(t)dt. \tag{9}$$

Clearly, in the absence of direct interactions between the Brownian particles, $\mathbf{F}^{\text{int}}=0$, $\Delta\zeta(t)=0$, and $V(t)=\exp[-t/\tau_B]$, where $\tau_B\equiv M/\zeta^0$. Since we are only interested in describing self-diffusion in the diffusive regime, $t\gg\tau_B$, we shall neglect terms of order (τ_B/t) or, equivalently, terms of order $(z\tau_B)$ in Eq. (7). This corresponds to the so-called overdamped limit.[3] In this limit, we may write Eq. (7) as

$$\tilde{V}(z)=\frac{k_BT}{\zeta^0+\Delta\tilde{\zeta}(z)}. \tag{10}$$

Thus, if we know $\Delta\zeta(t)$, we could use Eq. (10) to calculate $V(t)$, and Eq. (3) to calculate $D(t)$. This is the approach we shall use in the context of one of the dynamic theories considered in this work.[10]

An alternative approach to calculate $D(t)$ makes use of an exact expression for this quantity in terms of another fundamental property describing self-diffusion, namely, the self-diffusion propagator

$$G_s(k,t)\equiv\langle e^{i\mathbf{k}\cdot\Delta\mathbf{r}(t)}\rangle. \tag{11}$$

This function satisfies the following time-evolution equation:[1]

$$\frac{\partial G_s(k,t)}{\partial t}=-k^2D_0G_s(k,t)+\int_0^t dt'\,M(k,t-t')G_s(k,t'), \tag{12}$$

in which the memory function $M(k,t)$ represents the departures from free diffusion due to direct interactions. From Eqs. (11) and (12), and from the definition of $D(t)$, one can show that $D(t)$ can be written as

$$D(t)=D_0-\int_0^t dt'[1-t'/t]\lim_{k\to0}\left(\frac{M(k,t')}{k^2}\right). \tag{13}$$

Thus if we had a theory that allowed us to calculate the memory function $M(k,t)$, this equation can be used to calculate $D(t)$. This will be done here in the context of the second dynamic theory considered.[4]

A. Generalized Langevin equation and the decoupling approximation

In the previous work of M.M.-N.,[11] a general expression was derived for the time-dependent friction function $\Delta\zeta(t)$ [see Eq. (4.10) of Ref. 11]. If one follows such derivation, which refers to three-dimensional systems, one finds that it is a rather simple exercise to translate each step of the derivation to the two-dimensional context. Thus, one finds that in our case, $\Delta\zeta(t)$ can be written as

$$\Delta\zeta(t)=\frac{k_BT}{2}\int d^2r_1\int d^2r_2\int d^2r_3[\nabla n^{\text{eq}}(r_1)]\times\sigma^{-1}(\mathbf{r}_1,\mathbf{r}_2)\chi'(\mathbf{r}_2,\mathbf{r}_3;t)[\nabla n^{\text{eq}}(r_3)] \tag{14}$$

[which is the two-dimensional version of Eq. (4.13) of Ref. 11]. In this equation, $n^{\text{eq}}(r)$ is the local concentration of Brownian particles around the tracer, i.e.,

$$n^{\text{eq}}(r)=ng(r), \tag{15}$$

where $g(r)$ is the radial distribution function, $\sigma^{-1}(\mathbf{r},\mathbf{r}')$ is the inverse function of the static correlation of the fluctuations in the local concentration of Brownian particles,

$$\sigma(\mathbf{r},\mathbf{r}')\equiv\langle\delta n(\mathbf{r})\,\delta n(\mathbf{r}')\rangle=n^{\text{eq}}(r)\,\delta(\mathbf{r}-\mathbf{r}')+n^{\text{eq}}(r)n^{\text{eq}}(r')h^{(2)}(\mathbf{r},\mathbf{r}'), \tag{16}$$

where $h^{(2)}(\mathbf{r},\mathbf{r}')\equiv g^{(2)}(\mathbf{r},\mathbf{r}')-1$, $g^{(2)}(\mathbf{r},\mathbf{r}')$ being the pair correlation function of the particles diffusing around the tracer in the field of this labeled particle [thus, $g^{(2)}(\mathbf{r},\mathbf{r}')$ is in reality a three-particle correlation function]. Finally, $\chi'(\mathbf{r},\mathbf{r}';t)$ is the collective diffusion propagator of the particles around the tracer, and as observed from a reference frame fixed to the tracer (which undergoes Brownian motion). Just as argued in Ref. 11, there is the need of approximations. The first of them refers to neglecting the inhomogeneity and anisotropy of $\sigma(\mathbf{r},\mathbf{r}')$ and $\chi'(\mathbf{r},\mathbf{r}';t)$ produced by the field of the tracer. This allows us to approximate $g^{(2)}(\mathbf{r},\mathbf{r}')$ by the radial distribution function $g(|\mathbf{r}-\mathbf{r}'|)$, and $\chi'(\mathbf{r},\mathbf{r}';t)$ by $\chi'(|\mathbf{r}-\mathbf{r}'|;t)$. As a result, one can rewrite Eq. (14) as

$$\Delta\zeta(t)=\frac{k_BTn}{2(2\pi)^2}\int d^2k\,\frac{[kh(k)]^2}{1+nh(k)}\,\chi'(k,t), \tag{17}$$

where $h(k)$ is the Fourier transform (FT) of $h(r)$,

$$h(k)=\int d^2r\,e^{i\mathbf{k}\cdot\mathbf{r}}h(r) \tag{18}$$

and $\chi'(k,t)$ being the FT of $\chi'(|\mathbf{r}-\mathbf{r}'|;t)$. Equation (17) is the analog of Eq. (4.14) of Ref. 11. Also, following the arguments in this reference, $\chi'(k,t)$ can be approximated by

$$\chi'(k,t)=G_s(k,t)\chi(k,t), \tag{19}$$

where $\chi(k,t)$ is the collective diffusion propagator of the bulk suspension and from the laboratory-fixed reference frame. Equation (19) embodies what we refer to[12] as the *decoupling approximation*, in reference to the rationale that suggested it. Finally, here we also adopt the short-time approximation for $G_s(k,t)$ and $\chi(k,t)$, namely,

$$G_s(k,t)\approx e^{-k^2D_0t} \tag{20}$$

and

$$\chi(k,t)\approx e^{-k^2D_0t/[1+nh(k)]}. \tag{21}$$

The latter approximation can also be arrived at by using Fick's diffusion law. Putting together Eqs. (17), (19), (20), and (21), we finally get the following approximate expression for $\Delta\zeta(t)$:

$$\Delta\zeta(t)=\frac{k_BTn}{4\pi}\int_0^\infty dk\,\frac{k^3h^2(k)}{1+nh(k)}\,e^{-k^2D_0t\{1+1/[1+nh(k)]\}}. \tag{22}$$

This equation writes $\Delta\zeta(t)$ in terms of only $h(k)$, a static property that must be calculated using statistical thermodynamic methods.

Let us point out that the three-dimensional analog of this expression for $\Delta\zeta(t)$, derived in Ref. 11, is identical to a result of Hess and Klein's work,[3] based on the mode–mode coupling (MMC) approximation. For that reason, in Ref. 11, it was referred to as the MMC approximation. To establish the necessary distinction between the two approaches leading to the same result, we shall refer to Eq. (22) as the *Fick plus decoupling approximation* (FDA) for $\Delta\zeta(t)$, in reference to the use of Eqs. (19)–(21) in its derivation. Let us also mention that the three-dimensional analog of this approximation was studied by Nägele *et al.*[5] Some details concerning the numerical procedure are explained in that paper. Here we only provide a brief summary.

The Laplace transform $\Delta\tilde{\zeta}(z)$ of Eq. (22), needed in Eq. (10) to get $\tilde{V}(z)$, is

$$\Delta\tilde{\zeta}(z)=\frac{k_BTn}{4\pi}\int_0^\infty dk\,\frac{k^3h^2(k)}{1+nh(k)}\,\frac{1}{z+k^2D_0\left(1+\dfrac{1}{1+nh(k)}\right)}. \tag{23}$$

The Laplace inverse of $\tilde{V}(z)$, now used in Eq. (3), would allow us to calculate $D(t)$. In practice, however, it is more convenient to calculate

$$f_c(w)\equiv\mathrm{Re}\;\Delta\tilde{\zeta}(-iw)/\zeta^0 \tag{24}$$

and

$$f_s(w)\equiv\mathrm{Im}\;\Delta\tilde{\zeta}(-iw)/\zeta^0, \tag{25}$$

in terms of which one writes $V(t)$ and $D(t)$ as

$$V(t)=D_0\delta(t)+\frac{2D_0}{\pi}\int_0^\infty dw\,\sin wt\;y_s(w) \tag{26}$$

and

$$\frac{D(t)}{D_0}=1-\frac{2t}{\pi}\int_0^\infty dw\,\frac{wt-\sin wt}{(wt)^2}\,y_s(w), \tag{27}$$

with

$$y_s(w)\equiv\frac{f_s(w)}{[f_s(w)]^2+[1+f_c(w)]^2}. \tag{28}$$

Additional details of these numerical aspects, are identical to those described in Appendix A of Ref. 5.

B. Single-exponential approximation

The second theory of self-diffusion that we shall consider is the two-dimensional version of the single-exponential memory function approximation (SEXP), suggested by Arauz-Lara,[4] and discussed by Nägele *et al.* In this theory, the basic concept is the self-diffusion propagator, $G_s(k,t)$, whose time-evolution equation is Eq. (12). This equation can be derived from the many-particle Smoluchowski equation, using projection operator techniques.[13] This results is a formally exact expression for the memory function $M(k,t)$, whose direct evaluation is not, however, a practicable task. One may instead take a more pragmatic attitude, in which a simple analytic functional form is assumed for its time decay. The simplest two-parameter model is a single exponential, whose amplitude and decay time are related to the initial values of $M(k,t)$ and of its time derivative [the first two "moments" of $M(k,t)$]. These moments are related, in its turn, to the first three moments of $G_s(k,t)$.

For three-dimensional systems, exact expressions (or "sum rules") exist[14] in terms of integrals involving the pair potential $u(r)$ between the Brownian particles and the two- and three-particle distribution functions. As a result, one can express the memory function, within this model, in terms of these integrals involving only static properties. The details of this proposal and the necessary derivations in the three-dimensional case can be consulted in Ref. 5. Here, again, it is not difficult to check that the two-dimensional version is quite similar, and the end result for $M(k,t)$ is

$$M(k,t)=[k^2(D_0)^2n\beta A]e^{-D_0t[k^2+\beta(2B+nc)/A]} \tag{29}$$

where

$$A(k)\equiv\int d^2r\;g(r)(\hat{\mathbf{k}}\cdot\boldsymbol{\nabla})^2u(r), \tag{30}$$

$$B(k)\equiv\int d^2r\;g(r)[(\hat{\mathbf{k}}\cdot\boldsymbol{\nabla})\boldsymbol{\nabla}u(r)]^2, \tag{31}$$

and

$$C(k)\equiv\int d^2r\,d^2r'\;g^{(3)}(\mathbf{r},\mathbf{r}')(\hat{\mathbf{k}}\cdot\boldsymbol{\nabla})(\hat{\mathbf{k}}\cdot\boldsymbol{\nabla}')\times(\boldsymbol{\nabla}\cdot\boldsymbol{\nabla}')u(r)u(r'), \tag{32}$$

where $g^{(3)}(\mathbf{r},\mathbf{r}')$ is the three-particle correlation function. Using Eq. (13), one can express $D(t)$ in terms of these integrals, and the result can be written rather simply as

$$\frac{D(t)}{D_0}=\frac{D_s}{D_0}-\left(\frac{D_s}{D_0}-1\right)(1-e^{-t/\tau})\,\frac{\tau}{t}, \tag{33}$$

where D_s is the (long-time) self-diffusion coefficient, given by

$$\frac{D_s}{D_0}=1-(D_0n\beta A)\tau \tag{34}$$

and τ is the decay time of $D(t)$, given by

$$\tau=\frac{A}{\beta D_0(2B+nC)}. \tag{35}$$

In summary, Eqs. (30)–(35) express $D(t)$ and D_s in terms of the static properties $u(r)$, $g(r)$, and $g^{(3)}(\mathbf{r},\mathbf{r}')$. Here we shall apply this approximate scheme, in a similar manner as it was done for three dimensions.[5] Just as in that application, we shall also introduce in our specific calculations, an

additional simplification, namely, we shall neglect the terms involving the three-body correlation function $g^{(3)}(\mathbf{r},\mathbf{r}')$, i.e., we shall set $nC \approx 0$ in Eqs. (33)–(35).

The specific results for $D(t)$ of this two-dimensional version of the SEXP approximation, together with the results of the decoupling approximation, and the BD calculations will be shown in Sec. IV.

C. Brownian dynamics simulations

The BD algorithm, as proposed by Ermark,[15] is based on the solution of the generalized N-particle diffusion equation. It defines an accurate procedure to calculate static and dynamic properties of a system of interacting Brownian particles. Within this algorithm, assuming specific statistical properties of the random forces due to the solvent, the displacement of the ith Brownian particle during a time interval Δt is given by

$$\mathbf{r}_i(t+\Delta t)-\mathbf{r}_i(t)=\mathbf{R}_i(\Delta t)+\beta D_0 \mathbf{F}_i^{\text{int}} \Delta t, \tag{36}$$

where D_0 is the free-particle diffusion coefficient (i.e., the diffusion coefficient in the absence of interparticle interactions), and $\mathbf{R}_i(\Delta t)$ is a random Gaussian displacement of the particle due to solvent–particle interactions, which is assumed to have zero mean and variance given by $4D_0\Delta t$. The force $\mathbf{F}_i^{\text{int}}$ in this equation arises from the direct interactions of the ith particle with the other Brownian particles in the system. This force can be computed once the pair potential is defined. In Eq. (36) Δt (the time step) is assumed to be short enough, in such a manner that the change in particles configuration does not lead to a large change in $\mathbf{F}_i^{\text{int}}$, so that this force can be taken as constant during this time step.

Initially, N (=400) particles are placed in a squared lattice array enclosed in a square box of length $L=(N/n)^{1/2}$. The particles are then allowed to move according to Eq. (36) until equilibrium is reached (about 15 000 time steps). The convergence of the average configurational potential energy of the system to a constant value is used as the equilibration criterion. The time step Δt between configurations is taken as a fraction of the "collision" time between particles, $\tau_l \equiv l^2/4D_0 = t_0/4n^*$, where $l=n^{-1/2}$ is the mean interparticle distance, $t_0=\sigma^2/D_0$, and $n^*=n\sigma^2$, with σ the particle's diameter. In our calculations we have used $\Delta t = 10^{-3}\tau_l$. In practice, we use a dimensionless time step $\Delta t^* \equiv \Delta t/t_0$, which was thus taken as $\Delta t^* = 10^{-3}\tau_l/t_0$ $(=10^{-3}/4n^*)$. In order to minimize edge effects, due to the finite size of the simulation system, we use conventional periodic boundary conditions.[16] The interaction potential is approximately zero above a certain distance r_c. Thus, for each particle we only consider its interaction with those other particles lying within a distance r_c from that given particle. After equilibrium is reached, we generate 5000 configurations, from which averages are computed. However, we only use 500 of them to actually calculate the radial distribution function, i.e., configurations are recorded only every ten time steps. This is to let the colloidal particles move appreciably so that the saved configurations are significantly different from each other. From the recorded configurations, the average radial distribution function is calculated by standard procedures.[16] As for the mean squared displacement, the average was taken by comparing the position of a given particle at a certain initial configuration, with its position a time t later. First, an ensemble average was taken, by considering each of the N particles of the system as the tracer particle. Second, a time average was also performed, by taking as many different initial configurations as possible. This, of course, was only possible for correlation times smaller than the total "experimental" time (i.e., that corresponding to the 5000 configurations generated after equilibration). As a result, the statistics corresponding to the short times are more accurate than at long times. The results presented below are restricted, however, to short and intermediate times, where those statistical uncertainties are still not appreciable.

III. MODEL SYSTEM AND STATIC STRUCTURE

The model system we refer to is composed of N particles in a surface S, interacting through a pairwise potential given by

$$\beta u(r)=\begin{cases} K\dfrac{e^{-z(r/\sigma-1)}}{\dfrac{r}{\sigma}}, & \dfrac{r}{\sigma}>1 \\ \infty, & \dfrac{r}{\sigma}<1 \end{cases}, \tag{37}$$

where σ is the hard-disk diameter, and K and z are the dimensionless coupling and screening parameters, respectively. We shall only refer to the dimensionless parameters K, z, and $n^* \equiv n\sigma^2$ where $n=N/S$. The numerical values employed for these parameters correspond roughly to a typical (three-dimensional) dilute suspension of charged spherical polystyrene spheres in aqueous solution at low ionic strength.[1]

The rest of this section is devoted to the discussion of the static properties of the two-dimensional model Brownian liquid just defined. Using the BD algorithm we have explored the parameter space of our system by chosing values of the dimensionless parameters K, z, and n^*, representative of weakly screened potentials ($z=0.15$), at moderate and high couplings ($100 \leqslant K \leqslant 1000$), and low concentrations ($0.003 \leqslant n^* \leqslant 0.009$). Let us first illustrate the effect of increasing K, at fixed density ($n^*=0.007$), on the radial distribution function $g(r)$. This is done in Fig. 1, which shows the radial distribution function for three different values of K (100, 500, and 1000). The main effect of increasing K is to emphasize the structure, represented by the maxima and minima of $g(r)$, without a considerable shift in the position of the first peak of $g(r)$ for strongly repulsive systems ($K=500$ and 1000), but with deviations of this behavior at smaller couplings ($K=100$). In Fig. 1 we can also observe an interesting feature of the structure of the system, which is due to the strongly repulsive Yukawa potential. Each Brownian particle has a mean kinetic energy, k_BT. If this energy is much smaller than the energy at contact (i.e., if $K \gg 1$), then two particles cannot come closer than an effective radial distance of closest approach between them. This allows us to define an effective diameter, σ', as the distance where $g(r)$ first departs appreciably from zero. As we can see from Fig. 1, σ' will increase if we increase the coupling parameter K.

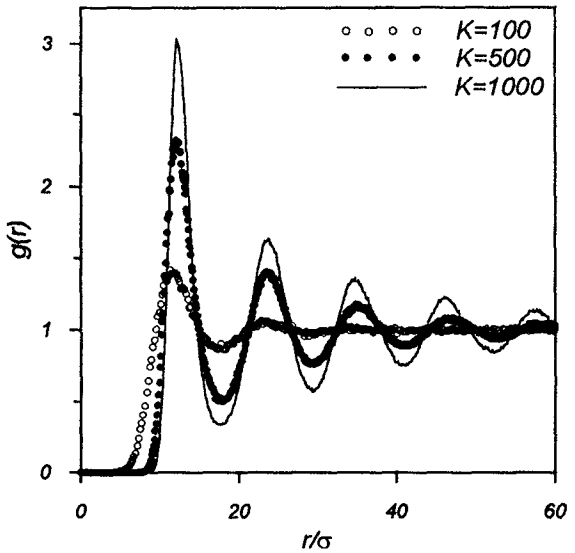

FIG. 1. Radial distribution function of the two-dimensional hard-disk plus Yukawa fluid at reduced density $n^*=0.007$, screening constant $z=0.15$, and Yukawa amplitude $K=100$ (open circles), 500 (closed circles), and 1000 (solid line). As is observed, increasing the interaction between particles, at fixed concentration, increases the local structure of the system without an appreciable change in the position of the first maximum.

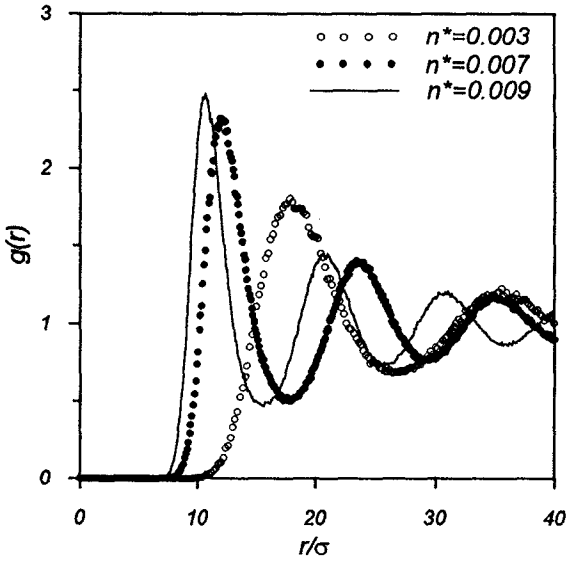

FIG. 2. Effect on the radial distribution function of increasing the reduced density n^* at fixed screening constant $z=0.15$, and Yukawa amplitude $K=500$.

The presence of this effective diameter implies that any system with hard-disk diameter smaller than σ', but with the same Yukawa tail, will have the same structure. This observation, in the three-dimensional context, gave rise to the "rescaling" argument behind the so-called rescaled mean spherical approximation (RMSA).[17] Our present computer simulation results exhibit, of course, the same rescaling feature, expected from any exact description of the structural properties of the model.

The dependence of $g(r)$ on the reduced density at fixed z $(=0.15)$, and K $(=500)$ is illustrated in Fig. 2. From this figure we can observe that the system has more structure as the reduced density is increased, and that the position of the maxima and minima of $g(r)$, are clearly dependent on n^*. As one can expect, the effective diameter decreases when the system is compressed.

For three-dimensional repulsive Yukawa systems, it has been observed that the position of the main peak of the static structure factor depends on the density in a very well defined fashion. Thus, the wave vector $k_{\max}$ is associated to the mean interparticle distance $l\equiv n^{-1/3}$ by $k_{\max}\approx 2\pi/l$. We found a similar behavior for the two-dimensional Yukawa system studied here. In Fig. 3 we show a sequence of structure factors, corresponding to various densities $(0.003\leqslant n^*\leqslant 0.009)$ at a fixed value of K $(=500)$. Clearly, the position $k_{\max}$ of the first peak moves to the right as n^* increases. In Fig. 4 we plot $k_{\max}$ as a function of n^*. From this plot we find that $k_{\max}$ depends on n^* as $\sigma k_{\max}=cn^{*s}$ with $c=6.52$ and $s=0.499$. Thus, the relationship $k_{\max}\approx 2\pi/l$ is also followed by the two-dimensional repulsive Yukawa fluid.

From the results in Figs. 1–4, we conclude that in general the two-dimensional system presents qualitatively the same structural features as its three-dimensional counterpart. However, it is also interesting to contrast the structure of the same system in two and in three dimensions. In Fig. 5 we present the radial distribution function of the hard-disk plus Yukawa and of the hard-sphere plus Yukawa fluids, for the same K $(=1000)$, z $(=0.15)$, and the same mean interparticle

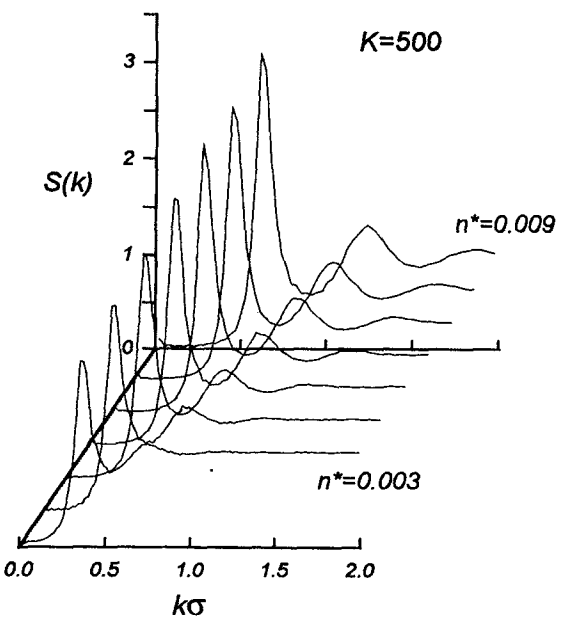

FIG. 3. Static Structure Factors for $K=500$, $z=0.15$, and reduced density ranging from 0.003 to 0.009. As is observed, there is a strong dependence of $k_{\max}$ on the reduced density n^*.

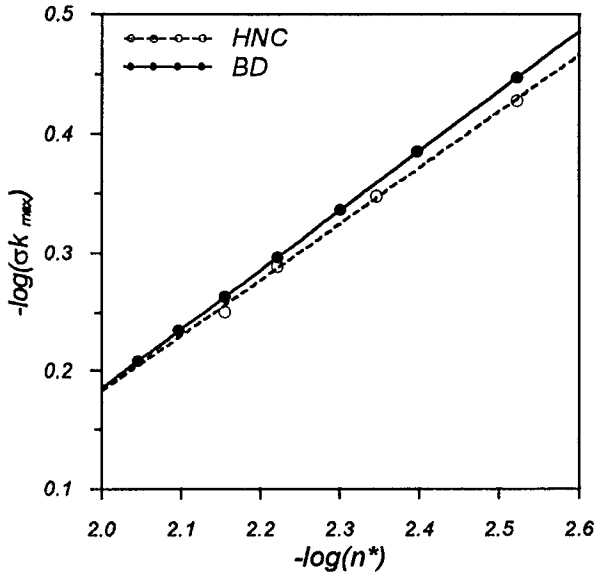

FIG. 4. (σk_{max}) as a function of reduced density (n^*) for $z=0.15$ and $K=500$, according to BD (solid circles) and HNC (open circles). The solid line (of slope 0.50) is a fit of the BD results for $n^* \geq 0.003$, and the dashed line is the corresponding fit of the HNC results, yielding a slope of 0.47.

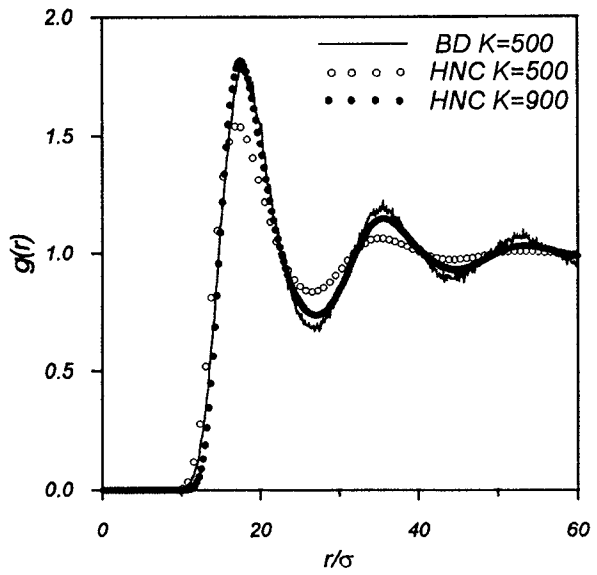

FIG. 6. Comparison between HNC (open circles) and BD (solid line) results for $g(r)$ corresponding to $z=0.15$, $n^*=0.003$, and $K=500$. Dots correspond to HNC calculations where the value of K has been adjusted to match the height of the first peak of the BD data for $g(r)$.

distance l $(=18.26\sigma)$, corresponding to $n^*=0.003$ for the two-dimensional case, and to $n^* \equiv n\sigma^3 = 1.643 \times 10^{-4}$ for three dimensions. As we see from Fig. 5, in both cases, the effective diameter, σ', is roughly the same $(\sigma' \approx 13\sigma)$, but the two-dimensional system is clearly more structured than its three-dimensional counterpart.

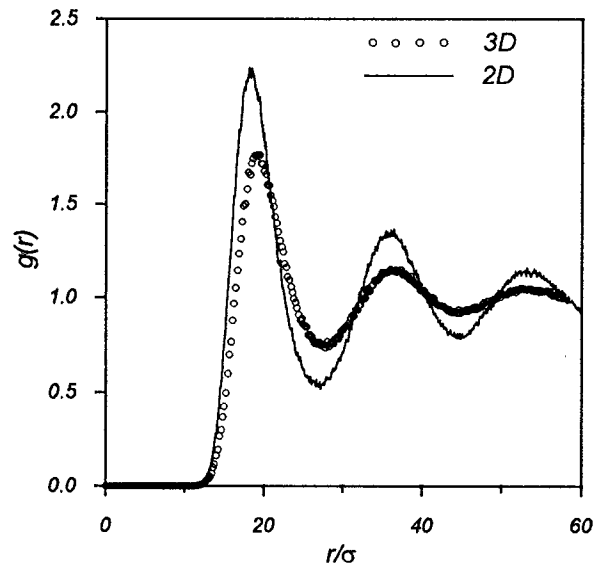

FIG. 5. The radial distribution function of the two- and three-dimensional hard-core plus Yukawa fluids, as calculated within the BD simulations, for a Yukawa amplitude $K=1000$, screening constant $z=0.15$, and $n^* = n\sigma^2 = 0.003$ (two dimensions, solid line), and $n^* = n\sigma^3 = 1.64 \times 10^{-4}$ (three dimensions, open circles). The mean interparticle distance in both cases is 18.26σ.

The discussion above describes the general features of the structural properties of the hard-disk plus Yukawa fluid, as drawn from our computer simulation results. In recent work,[18] we have presented a similar study based on an approximate theory, namely, the solution of the Ornstein–Zernike integral equation within the HNC closure. The results of those calculations also revealed general features of the static structure of the system, all of which are being confirmed by our present simulation results. For example, according to the previous HNC results, we also observed that the system becomes more structured when we increase K at fixed n^* and z, and when we increase n^* keeping K and z constant. Also, the relationship between the HNC results for k_{max} and n^* follows the power law discussed above, with values for c and s (see Fig. 4) of 5.74 and 0.47, respectively. Similarly, the rescaling property of $g(r)$ is also accurately predicted by the HNC results. Thus, we can state that this general scenario, provided before by this approximate theory, is now being confirmed to be qualitatively correct, according to our present BD results. It is then instructive to illustrate the degree of *quantitative* accuracy of the HNC results. One aspect of this comparison was already presented in Fig. 4 for k_{max}. However, the direct comparison of the HNC and BD results for $g(r)$ at a typical state of the system is also illustrative. This is done in Fig. 6, for a system with $K=500$, $z=0.15$, and $n^*=0.003$. From this figure we can see that the position of the maxima and minima of $g(r)$ are accurately predicted, along with the size of the effective diameter. The quantitative disagreement between the HNC and the BD results observed in Fig. 6 is most apparent in the height of the maxima and minima of $g(r)$, which in the HNC results are notoriously less pronounced. The structural properties provided by the HNC results could also be used as the static input needed to calculate self-diffusion quantities, according

to the results of the two dynamic theories described above. This would lead to an approximate scheme in which the only input is the pair interparticle potential. The results of this combined theory, however, will also combine the inaccuracies of the static (the HNC approximation) and of the dynamic theories. We have calculated the mean squared displacement of our system in this manner, and the general observation is that the qualitative predictions are indeed generally correct. However, in order to isolate the quantitative effect of the approximations involved in the dynamic theories only, here we shall report results in which the exact (i.e., computer simulated) structure is employed as such a static input. For completeness, however, let us mention, that the HNC structure calculated for the same z and n^* as the simulation data, but with a given larger value of K, say K_{ef}, happens to fit reasonably well the first peak of the simulated $g(r)$ for n^*, z, and K. This is also illustrated in Fig. 6, with $K_{ef}=900$. A similar observation was made in the context of the three-dimensional hard-sphere plus Yukawa fluid and the RMSA.[5] This observation summarizes a general conclusion of the comparison of the HNC results for $g(r)$ with our present BD data, namely, that for a given state (i.e., for a given set of value of z, n^*, and K), the features observed in the BD data are generally reproduced by the HNC results, although at a different state. Recalling a similar comparison made before for the three-dimensional case,[5] one can state that the quantitative disagreement between the two theories and the BD results are indeed not larger in the present case.

IV. SELF-DIFFUSION

In this section we present the theoretical results of the two independent approximations discussed in Sec. II, for the self-diffusion properties of our two-dimensional model suspension. We also present the BD computer simulation results for the quantity of interest, namely, the time-dependent self-diffusion coefficient $D(t)$. Since the static structure, characterized by $g(r)$ or $S(\mathbf{k})$, is also determined by n^* and $u(r)$, the self-diffusion properties of highly dilute but strongly coupled systems depend basically only on these two quantities. More specifically, our model system is characterized by n^*, K and z. As in the previous section, to minimize the number of parameters to be varied, we keep fixed the value of $z(=0.15)$, and we vary only n^* and K.

For simplicity, we first present separately the results for $D(t)$ from the three approaches, in order to get a better insight on the qualitative behavior for $D(t)$, as predicted by the FDA and SEXP approximations, and calculated by BD. Later on, a quantitative comparison of the three approaches is done for selected values of n^* and K. Thus, in Figs. 7–9, $D(t)$ is plotted as a function of time for various values of the reduced concentration ($n^*\times 10^3=3$–9), keeping fixed the parameters of the pair potential, $K=500$ and $z=0.15$. Figures 7–9 show the results of of the FDA [Eq. (27)] and SEXP [Eq. (33)] approximations and of the BD simulations, respectively. In order to evaluate Eqs. (27) and (33), we require as input the radial distribution functions and the static structure factors of these systems. In our calculations of $D(t)$ we used the values of $g(r)$ and $S(k)$ generated by the BD simulation (see the previous section). In Figs. 7 and 8 one can see that

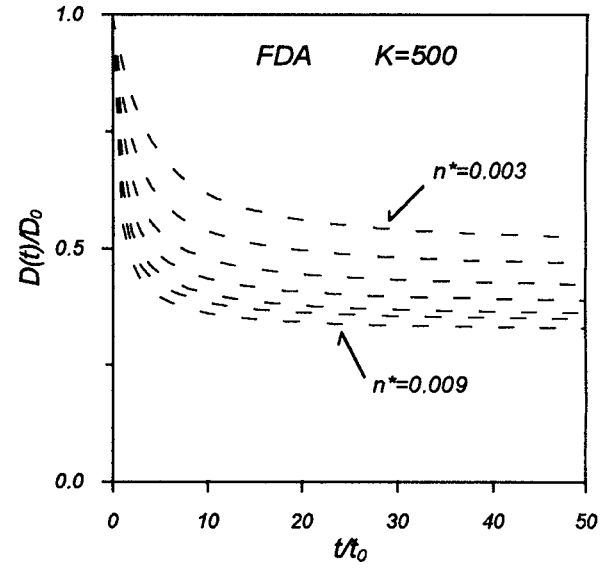

FIG. 7. FDA results for the time-dependent self-diffusion coefficient corresponding to a system with $K=500$, $z=0.15$, and reduced density from 0.003 to 0.009.

both theoretical approximations predict the same general trends in the behavior for $D(t)$, for the various concentrations, and that they also agree qualitatively with the BD results. In particular, in the three sets of results, the fastest decay of $D(t)$ from its initial value D_0 towards its asymptotic limit D_s occurs in the short-time regime, within a similar time interval, which for the particular systems in Figs. 7 and 8 is of the order of $10t_0$. After this rather rapid initial decay, $D(t)$ continues to drop much more slowly. It is im-

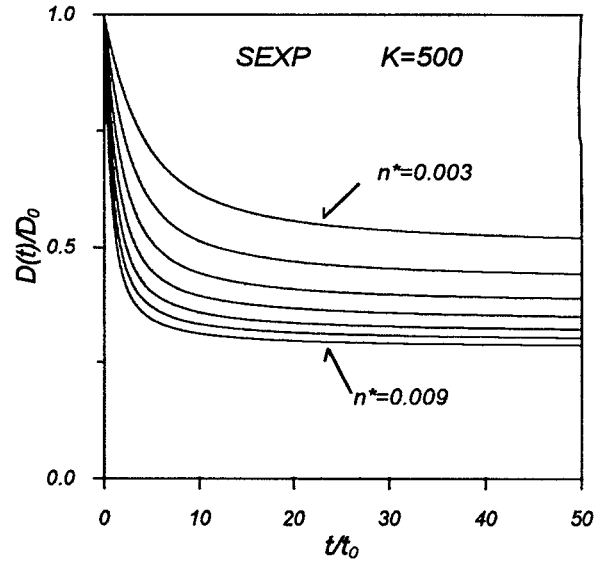

FIG. 8. SEXP results for the time-dependent self-diffusion coefficients corresponding to the systems in Fig. 7.

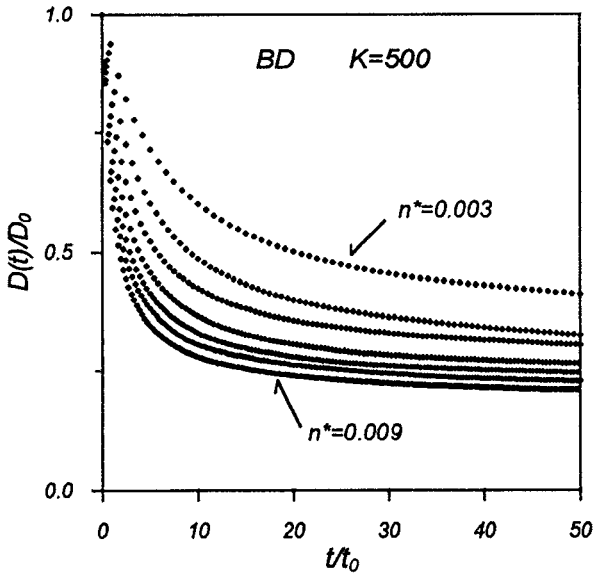

FIG. 9. BD results for the time-dependent self-diffusion coefficients corresponding to the systems in Fig. 7.

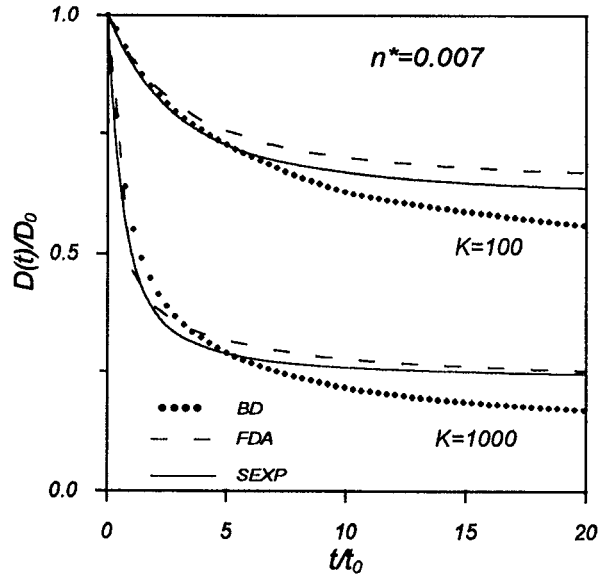

FIG. 11. Same comparison of $D(t)$ from the FDA, SEXP, and the BD calculations as in Fig. 10. Here $n^*=0.007$, $z=0.15$, $K=100$, and $K=1000$.

portant to notice the magnitude of the decay of $D(t)$, which after this initial fast relaxation, decays to values smaller or around 0.5 D_0. This means that the systems considered are very highly coupled. There are, however, quantitative differences, between the two theoretical predictions and the BD results. They are more pronounced between the two theories and the computer simulation results. In order to illustrate these quantitative differences, in Figs. 10 and 11 we compare the results from the three approaches for $D(t)$ for the extreme values of n^* and K considered in this work. In Figs. 10 and 11 the BD results are represented by dots, the FDA by dashed lines, and the SEXP by solid lines. We can see in Figs. 10 and 11 that for the less coupled systems, both theoretical approximations agree very well, qualitatively and quantitatively, with the BD calculations at short times. At longer times, the predictions of both approximations deviate from the BD results, more markedly as the coupling of the system increases.

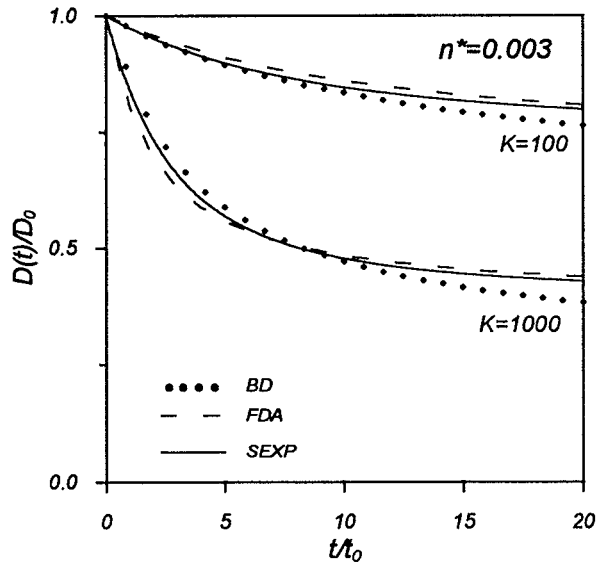

FIG. 10. Quantitative comparison of the predictions for $D(t)$ from the FDA (dashed lines) and SEXP (solid lines), and the BD calculations (dots), for systems with $n^*=0.003$, $z=0.15$, $K=100$ (three upper curves), and $K=1000$ (three lower curves).

Let us notice that one important feature of the curves in Figs. 7–11 is the initial slope of $D(t)$. This quantity is directly related to the spring constant of the locally harmonic potential well that a particle sitting in the middle of its average cage feels at very short times. This initial slope is given by the exact short-time condition[5]

$$-\frac{1}{D_0}\left(\frac{dD(t)}{dt}\right)_{t=0}=\frac{1}{2}D_0\beta n\int d^2r g(r)(\hat{\mathbf{k}}\cdot\nabla)^2u(r) \tag{38}$$

which is proportional to A, the integral given in Eq. (30). By construction, this condition is satisfied exactly by the SEXP approximation, and this is reflected in the numerical comparison in Figs. 10 and 11. The FDA on the other hand, does not satisfy exactly this short-time condition. Looking at Figs. 10 and 11, however, one observes that the numerical FDA results do satisfy this short-time condition very accurately. To understand this, let us notice that the initial slope of $D(t)$ is essentially the initial value of $\Delta\zeta(t)$, namely,

$$-\frac{1}{D_0}\left(\frac{dD(t)}{dt}\right)_{t=0}=\frac{\Delta\zeta(t=0)}{2\zeta^0}, \tag{39}$$

as can be shown using Eqs. (3) and (10). Within the FDA approximation, then the initial slope of $D(t)$ is given, using Eq. (17), by

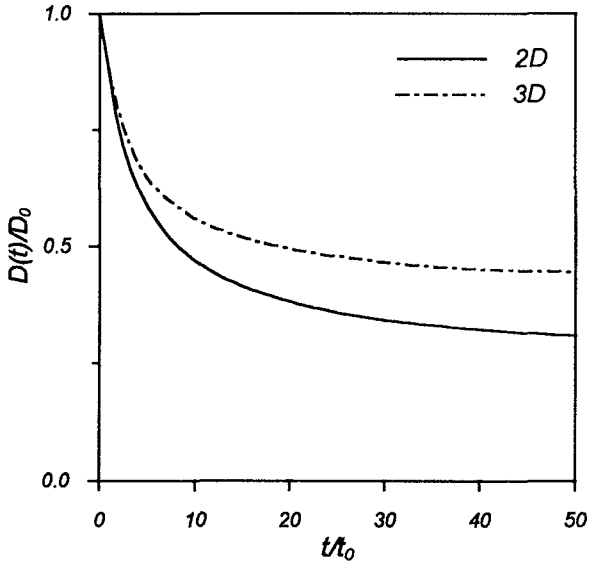

FIG. 12. Comparison of BD results for $D(t)$, for the two- and three-dimensional systems of Fig. 5. In both systems $K=1000$, $z=0.15$, and the mean interparticle distance is 18.16σ [which corresponds to $n^*=n\sigma^2=0.003$ for two-dimensions (solid line), and $n^*=n\sigma^3=1.64\times10^{-4}$ for three dimensions (dashed-dotted line)].

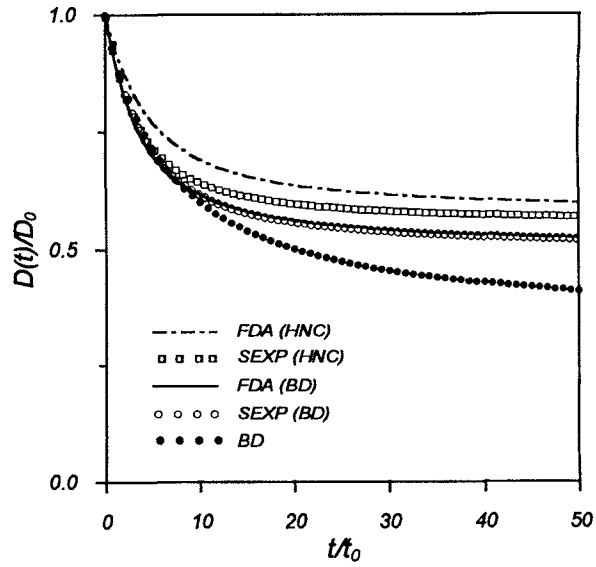

FIG. 13. Comparison of the time-dependent self-diffusion coefficient, for the system with $K=500$, $n^*=0.003$, and $z=0.15$, calculated using exact (BD) and approximated (HNC) results for the static properties as input in the dynamic theories FDA (dashed-dotted and solid lines, respectively) and SEXP (squares and open circles, respectively). For comparison, exact (BD) data for $D(t)$ are also shown.

$$-\frac{1}{D_0}\left(\frac{dD(t)}{dt}\right)_{t=0}=\frac{1}{4}D_0 n\,\frac{1}{(2\pi)^2}\int d^2k\,\frac{k^2h^2(k)}{1+nh(k)} \tag{40}$$

which, using the Ornstein–Zernike equation,

$$C(k)=\frac{h(k)}{1+nh(k)}$$

along with Parseval's theorem, and integrating by parts, can also be written as

$$\frac{1}{D_0}\left(\frac{dD(t)}{dt}\right)_{t=0}=\frac{1}{2}D_0 n\int d^2r\; g(r)(\hat{\mathbf{k}}\cdot\nabla)^2c(r), \tag{41}$$

which is Eq. (38) with $\beta u(r)$ substituted by $-c(r)$. This then means that in the regime where $g(r)$ is nonzero, the departures of the direct correlation function $c(r)$ from its Debye–Hückel limit do not have a strong influence on the value of the initial slope. This is similar to what was observed in the three-dimensional case. At long times, larger quantitative inaccuracies are expected, and they are indeed observed in the results in Figs. 10 and 11.

Let us now compare the effect of dimensionality on the self-diffusion in the model studied here. Just as in Fig. 5, let us compare a two-dimensional vs a three-dimensional system that have in common the same mean interparticle distance. As expected from the fact that the 2D is more strongly correlated than its 3D counterpart, the self-diffusion coefficient is smaller for the 2D system, and in general the 2D tracer particle diffuses more slowly than its 3D counterpart at all times. This is illustrated in Fig. 12, where BD results for $D(t)$ are plotted for the systems in Fig. 5.

As a final remark, let us recall that the quantitative inaccuracies exhibited by the theoretical predictions, only derive from the approximate nature of the expressions for $D(t)$ corresponding to each theory. This is due to the use of the exact (i.e., computer simulated) $g(r)$ and $S(k)$ as the static input, instead of any approximate results for these properties, such as the HNC calculations referred to in the previous section. It is important to stress, however, that the dynamic results predicted by the two theories, when the HNC statics was employed, did not differ at all in the general trends illustrated in the results presented in this section. The disagreement is essentially quantitative. Figure 13 illustrates the magnitude of the additional quantitative inaccuracies introduced by the HNC statics in the calculation of the dynamics. In Fig. 13, $D(t)$ is calculated for the system in Fig. 6, using both HNC and BD, as the static input in the dynamical theories. For comparison, the BD results for $D(t)$ are also shown in Fig. 13. As one can see, the use of the HNC structure leads to an additional disagreement from the BD results for $D(t)$, of different magnitude for each theory. One can also observe that for this particular system, the results from FDA and SEXP concide quantitatively when the BD data for $S(k)$ and $g(r)$ are used as input, but this is accidental.

V. SUMMARY

In summary, in this report we have presented two theoretical approximations describing self-diffusion in two-dimensional colloidal suspensions, in terms of the static properties of the system. The main results of these approximations are expressions for quantities characterizing the single particle dynamics, such as the time-dependent self-

diffusion coefficient. It is interesting to notice that both expressions for $D(t)$, derived within completely different theoretical frameworks, lead to quite similar results, both qualitatively and quantitatively, in the case of the specific model system defined in Eq. (37), as shown in Figs. 7–11. Further, the comparison of both theoretical approximations with the BD results for $D(t)$, shows that for not too highly coupled systems, both theories provide an accurate microscopic description of the self-diffusion properties of the hard-disk plus Yukawa Brownian fluid studied here. We expect that for real systems, the theories discussed here will provide at least the same level of accuracy in the description of self-diffusion phenomena.

ACKNOWLEDGMENTS

This work was partially supported by the Consejo Nacional de Ciencia y Tecnología (CONACyT), México, through Grant Nos. E764, F0064, and 3882E and a fellowship to H.A.E. Two of us (M.M.-N. and H. A.-E.) also acknowledge the UCSB Materials Research Laboratory for its kind hospitality and partial support (Grant No. DMR-9123048).

[1] P. N. Pusey and R. J. A. Tough, in *Dynamic Light Scattering: Applications of Photon Correlation Spectroscopy*, edited by R. Pecora (Plenum, New York, 1985).

[2] P. N. Pusey, in *Liquids, Freezing and Glass Transition*, edited by J. P. Hansen, D. Levesque, and J. Zinn-Justin (North-Holland, Amsterdam, 1991).

[3] W. Hess and R. Klein, Adv. Phys. **32**, 173 (1983).

[4] (a) J. L. Arauz-Lara, thesis, CINVESTAV, México, 1985; (b) J. L. Arauz-Lara and M. Medina-Noyola, J. Phys. A. **19**, L117 (1986).

[5] G. Nägele, M. Medina-Noyola, R. Klein, and J. L. Arauz-Lara, Physica A **149**, 123 (1988).

[6] R. Krause, G. Nägele, D. Karrer, J. Scheneider, R. Klein, and R. Weber, Physica A **153**, 400 (1988).

[7] I. K. Snook, W. van Megen, K. J. Gaylor, and R. O. Watts, Adv. Colloid Interface Sci. **17**, 33 (1982).

[8] (a) R. Krause, J. L. Arauz-Lara, G. Nägele, H. Ruiz-Estrada, M. Medina-Noyola, R. Weber, and R. Klein, Physica A **178**, 241 (1991); (b) R. Krause, G. Nägele, J. L. Arauz-Lara, and R. Weber, J. Colloid Interface Sci. **148**, 231 (1992).

[9] (a) C. A. Murray and D. H. Van Winkle, Phys. Rev. Lett. **58**, 1200 (1987); (b) C. A. Murray and R. A. Wenk, *ibid.* **62**, 1643 (1989); (c) P. González-Mozuelos, J. Alejandre, and M. Medina-Noyola, J. Chem. Phys. **95**, 8337 (1991).

[10] H. Lowen, J. Phys. **4**, 10105 (1992).

[11] M. Medina-Noyola, Faraday Discuss. Chem. Soc. **83**, 21 (1987).

[12] G. Cruz de León, M. Medina-Noyola, O. Alarcon-Waess, and H. Ruiz-Estrada, Chem. Phys. Lett. **207**, 294 (1993).

[13] (a) B. J. Ackerson, J. Chem. Phys. **64**, 242 (1976); (b) **69**, 684 (1978).

[14] J. L. Arauz-Lara and M. Medina-Noyola, Physica A **122**, 547 (1983).

[15] D. L. Ermack, and Y. Yeh, Chem. Phys. Lett. **24**, 243 (1974).

[16] M. P. Allen and D. J. Tildesley, *Computer Simulation of Liquids*, 5th ed. (Oxford Science, New York, 1993).

[17] J. P. Hansen and J. B. Hayter, Mol. Phys. **46**, 651 (1982).

[18] H. Aranda-Espinoza, M. Medina-Noyola, and J. L. Arauz-Lara, J. Chem. Phys. **99**, 5462 (1993).